IEEE Access
Multidisciplinary ⋮ Rapid Review ⋮ Open Access Journal

Received April 17, 2022, accepted April 27, 2022, date of publication May 2, 2022, date of current version May 13, 2022.

Digital Object Identifier 10.1109/ACCESS.2022.3171909

Automatic Digital Modulation Recognition Based on Genetic-Algorithm-Optimized Machine Learning Models

SAM ANSARI[1], KHAWLA A. ALNAJJAR[1], (Member, IEEE), MOHAMED SAAD[2], (Senior Member, IEEE), SAEED ABDALLAH[1], (Member, IEEE), AND ALI A. EL-MOURSY[2], (Senior Member, IEEE)

[1]Department of Electrical Engineering, University of Sharjah, Sharjah, United Arab Emirates
[2]Department of Computer Engineering, University of Sharjah, Sharjah, United Arab Emirates

Corresponding author: Khawla A. Alnajjar (kalnajjar@sharjah.ac.ae)

ABSTRACT Recognition of the modulation scheme is the intermediate step between signal detection and demodulation of the received signal in communication networks. Automatic modulation recognition (AMR) plays a central role in many applications, especially in the military and security sectors. In general, several properties of the received signal are extracted and employed for AMR. Selecting the appropriate features has a significant impact on increasing the efficiency of AMR. In this paper, we implement and compare digital modulation recognition via multi-layer perceptrons (MLP), radial basis function (RBF), adaptive neuro-fuzzy inference system (ANFIS), decision tree (DT), and naïve Bayes (NB) algorithms. In addition, the optimal parameters of each model are obtained by utilizing a genetic algorithm (GA). A series of studies are conducted in this work in order to determine the efficiency of different algorithms in identifying modulated signals with commonly used digital modulations. Numerous computer simulations are performed in the presence of additive white Gaussian noise (AWGN) with a signal-to-noise ratio (SNR) ranging from −10 dB to 30 dB. The simulation results and comparisons with previous studies demonstrate that applying the proposed algorithms along with the selected features leads to a significant enhancement in the accuracy and speed of the automatic determination of the digital modulation types at low SNRs. In addition, the convergence rates of the models are enhanced.

INDEX TERMS Automatic modulation recognition, classification, feature extraction, genetic algorithm, machine learning.

I. INTRODUCTION

Automatic modulation recognition (AMR) is crucial for detecting and demodulating a telecommunication signal [1], [2]. AMR has attracted considerable attention owing to its wide range of applications. AMR is employed in electronic warfare (EW) systems as a source of information for detecting and disrupting threats [3]. Civilian applications include software-defined radio, frequency management, transmitter monitoring, and network traffic administration [4]–[7].

Two primary phases are considered in AMR: initial preprocessing of the input signal and selection of the classifier system. There are two approaches to performing AMR. One approach is decision-theoretic, and the other is statistical pattern recognition (i.e., feature-based pattern recognition) [8]. The former entails high computational complexity and suffers from the ambiguity of the parameters. In the second approach, certain features of the signal are extracted first. Then decisions are made based on the extracted characteristics. The latter is less complex compared to the first approach. Therefore, it is more convenient to implement the second approach in practical systems. In our work, we focus on the pattern recognition approach.

Numerous studies have proposed investigating different features to identify the types of modulation [9]. Hsue and Soliman [10] propose to utilize the frequency and phase histograms in addition to zero-crossing features and zero-crossing variance of the received signal for modulation

The associate editor coordinating the review of this manuscript and approving it for publication was Zahid Akhtar.

recognition purposes. The authors in [11] leverage frequency and amplitude variances and phase difference histogram to distinguish various digital modulation types. The work in [12], [13] use wavelet transform and wavelet features empowered by neural networks to recognize several modulation schemes. The study in [14] uses the signal spectrum's fourth power and the mean of the signal envelope and variance characteristics to classify various digitally modulated signals. Moreover, other spectral characteristics (i.e., frequency-based features), statistical attributes, e.g., higher-order statistics [15]–[17], together with instantaneous phase, frequency, and amplitude [16], [18] are further examined for AMR. We utilize six attributes, including the spectral, temporal, and wavelet-based features, to distinguish seven different digital modulation techniques.

Machine learning and optimization algorithms are continuously employed to provide accurate and reliable AMR. The feature-based study in [19] exploits support vector machine (SVM) algorithm to recognize four different digital modulation schemes, including binary phase-shift keying (BPSK), 8-PSK, 4-ary amplitude-shift keying (4-ASK), and 16-ary quadrature amplitude modulation (16-QAM). The work achieves an accuracy of 100% by investigating the two-dimensional asynchronous sampled in-phase-quadrature histograms (ASIQ) in the presence of additive white Gaussian noise (AWGN) with signal-to-noise ratio (SNRs) ranging from 0 dB to 35 dB. Genetic algorithm (GA) is one of the most well-known evolutionary algorithms used together with other machine learning models to further enhance AMR efficiency. Artificial neural networks (ANNs) and GA are used in [20] to distinguish various digital modulation techniques. An augmented genetic programming (GP) and the k-nearest neighbor (KNN) algorithm are employed in [21] to classify digital modulations. Zhang *et al.* [22], propose GP to generate features utilized by the KNN algorithm for multi-class modulation classification. Most implementations are based on neural network (NN) methods and GAs [21]–[24]. Almohamad *et al.* [25], utilize the SVM model to classify nine modulation types, including BPSK, QPSK, 8-PSK, BASK, 4-ASK, 4-QAM, 16-QAM, 32-QAM, and 64-QAM over AWGN and Rayleigh fading channels within a wide range of SNR values, i.e., 0 dB through 35 dB. Their proposed model simultaneously performs AMR and estimates SNRs values by exploring two-dimensional asynchronously sampled in-phase-quadrature amplitudes' histograms (2D-ASIQHs).

On the other hand, we see many efforts in recent work to employ deep learning methods in AMR [2]. In particular, the study in [26] proposes a novel technique based on the InceptionResNetV2 network with transfer adaptation to distinguish between three types of phase-shift keying (PSK) modulation, including BPSK, quadrature phase-shift-keying (QPSK), and 8-PSK. An average accuracy of 75.99% is achieved at SNR $=$ 1 dB. The work in [27] achieves 99.00% accuracy at low SNRs by employing a deep neural network (DNN) to extract different features of each modulation type by learning different cumulant combinations of ASK, frequency-shift keying (FSK), and PSK modulation schemes.

A long short-term memory network (LSTM) and a deep convolutional neural network (DCNN) are utilized in [28] to form an AMR system. The authors substitute the in-phase/quadrature (I/Q) information by exploiting high-order statistics (HOS), i.e., I/Q and fourth-order cumulants (FOC) which result in an average accuracy of roughly 80.00% at SNR $=$ 0 dB. Daldal *et al.* [29] designed an AMR system by employing CNN and the short-time Fourier transform (STFT) to recognize six distinct digital modulation schemes automatically. The system achieves an average accuracy of 99.19% for SNRs above 0 dB. A generalized CNN method is proposed in [30] to identify FSK, PSK, and QAM schemes robustly. The model is trained and utilized for both AWGN and Rayleigh fading channels.

Some of the existing AMR frameworks based on machine learning have been able to perform well in terms of accuracy. However, it has been observed that these models suffer from high computational complexity. The existing methods necessitate additional preprocessing procedures and possess more tuning parameters and classifiers, resulting in slower and larger hardware. In addition, their accuracy drops significantly at low SNRs. Consequently, their ability to generalize is limited. Therefore, our goal is to provide machine learning-based AMR frameworks with lower time complexity (i.e., the running time of the algorithms) and higher accuracy compared to existing methods, especially at low SNRs. In this paper, various digital modulations are identified and classified by employing multi-layer perceptrons (MLP), radial basis function (RBF), adaptive neuro-fuzzy inference system (ANFIS), decision tree (DT), and naïve Bayes (NB) algorithms. Additionally, a GA is employed to optimally select the tuning parameters to further enhance the proposed system. Our selected models result in significantly faster and more efficient AMR without compromising the accuracy.

In light of the above, the contributions of this paper are as follows.

- We leverage various machine learning algorithms to automatically recognize and classify different digital modulation schemes.
- We propose a heuristic optimization method, i.e., GA, to optimize the tunable parameters of presented machine learning algorithms that are employed to classify various digital modulation techniques.
- We investigate different features to classify different digital modulation techniques employing feature extraction-based approaches.
- We examine the accuracy of the employed models and perform exact and comprehensive comparisons based on different criteria, including accuracy, complexity, and time. Our model achieves an accuracy of 100% at SNR of -2 dB with significantly lower complexity (i.e., the running time of the algorithm) compared to existing

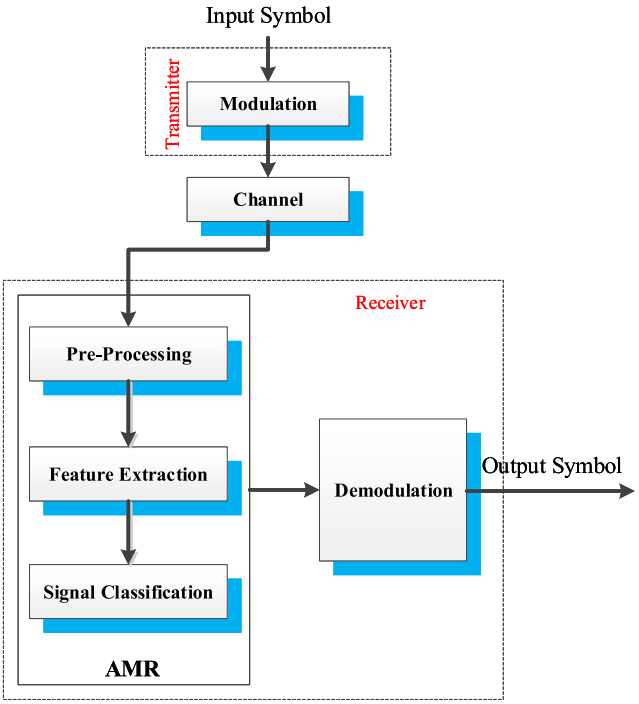

FIGURE 1. Schematic diagram of a simplified AMR system based on the pattern recognition method.

techniques. The obtained classification accuracy is justified by the utilization of 10-fold cross-validation.

The remainder of the paper is organized as follows. Section II introduces the system model and features exploited in this study. The machine learning algorithms employed for the AMR are presented in Section III. Simulation analyses are performed in Section IV. Finally, Section V provides a summary, conclusion, and avenues for future work.

II. SYSTEM MODEL AND SELECTED FEATURES

Without loss of generality, this study performs communication and signal transmission over the AWGN channel. The transmitter modulates the desired signals, which are then transmitted. After passing through the channel, the signal is mixed with white Gaussian noise. The transmitted signal enters the receiver block while no information is available from the sender. The input signal is modulated as follows [31]:

$$z(t) = \tilde{s}(t)\, e^{j(2\pi f_c t + \phi_c)} + n(t)\,, \tag{1a}$$

$$\tilde{s}(t) = a(t)\, e^{j[2\pi f(t) t + \phi(t)]}, \tag{1b}$$

where f_c indicates the carrier frequency, ϕ_c is the carrier phase, $n(t)$ represents the AWGN, and $\tilde{s}(t)$ designates the envelope of baseband signal. In (1b), $a(t)$, $f(t)$, and $\phi(t)$ represent the instantaneous amplitude, frequency, and phase of the signal, respectively.

Fig. 1 illustrates the modulation scheme classification system based on the pattern classification approach consisting of three subsystems. The preprocessing sub-block, upon the arrival of the intercepted modulated signal, prepares the received signal for the succeeding sub-block. The preprocessing operations include filtering to diminish the noise level, median filtering, estimating symbol length, signal power (i.e., SNR), carrier frequency, and balancing the received modulated signal. Besides, the instantaneous amplitude, frequency, and phase extraction are other parts of preprocessing framework. The processing operations enhance AMR performance. The selection of each task involved in preprocessing stage depends on the classification process.

One of the most critical tasks and perhaps the challenges when employing machine learning for AMR is selecting appropriate features. Equipping the system with suitable features allows us to identify and separate various modulation schemes accurately. In addition, given the instantaneous operation of AMR, it is essential to utilize features that significantly improve the operating speed of the model. It is crucial to use features that are robust against different signal and channel conditions such as SNR, frequency, etc. We employ the features of [32] and [9] to reinforce the presented machine learning algorithms for AMR to achieve superior robustness against low SNRs. Previous studies demonstrate that the selected features are among the most authentic attributes employed in the existing robust modulation recognition systems [8], [9]. In the following, we briefly examine the selected features and provide the mathematical expression of each.

The second-order moment of the non-linear component of the instantaneous phase is the first feature that we utilize in our AMR framework. The exact mathematical formula of this attribute is stated by [8]

$$M_{\varphi_{\mathrm{NL}}} = \frac{1}{N_s} \sum_{i=1}^{N_s} \varphi_{\mathrm{NL}}^2(i)\,, \tag{2a}$$

$$\varphi_{\mathrm{NL}}(i) = \frac{\varphi(i)}{\bar{\varphi}} - 1, \tag{2b}$$

where N_s is the number of symbols, $\varphi_{\mathrm{NL}}(i)$ indicates the normalized-center non-linear component of the instantaneous phase, $\varphi(i)$ denotes the instantaneous phase, and $\overline{\varphi}$ represents the mean phase. The instantaneous phase of the signals modulated by ASK contains no information, which causes the $M_{\varphi_{\mathrm{NL}}}$ values computed for the ASK modulated signals to be the lowest compared to that of other modulation schemes. Consequently, the intended trait accurately differentiates binary amplitude-shift keying (BASK) and 4-ASK modulations from QAM, PSK, and FSK modulations.

The spectrum-based feature is designated as the second characteristic employed in this work and is expressed by [8]

$$\sigma_z^2 = \frac{1}{N_s} \sum_{i=1}^{N_s} \left(Z(i) - \frac{1}{N_s} \sum_{i=1}^{N_s} Z(i) \right)^2, \tag{3}$$

where $Z(i)$ represents the discrete-time Fourier transform (DTFT) of the received signal. This feature can accurately distinguish ASK and QAM modulations from

other digital modulations schemes, including PSK and FSK modulations that possess no amplitude-related information.

The third attribute used in the proposed AMR system is the mean value of the power spectral density of the normalized-centered instantaneous amplitude of the intercepted signal segment, which is defined as [8]

$$\overline{\gamma} = \frac{1}{N_s}\sum_{i=1}^{N_s}|A_{cn}(i)|^2, \tag{4a}$$

$$a_{cn}(i) = \frac{a(i)}{m_a} - 1, \tag{4b}$$

$$m_a = \frac{1}{N_s}\sum_{i=1}^{N_s} a(i), \tag{4c}$$

where A_{cn} denotes the DTFT of the normalized-centered instantaneous amplitude, $a_{cn}(i)$ denotes the normalized-centered instantaneous amplitude, and m_a represents the mean value of instantaneous amplitude. The proposed AMR models of this study utilize this trait to detach 4-ASK modulation from BASK.

As our fourth feature, we select the standard deviation of the normalized-centered non-linear component of the direct instantaneous phase, containing phase-related information. The exact mathematical expression exploited to extract the attribute is [8]

$$\sigma_{dp} = \sqrt{\frac{1}{N_s}\left(\sum_{i=1}^{N_s}\varphi_{\mathrm{NL}}^2(i)\right) - \left(\frac{1}{N_s}\sum_{i=1}^{N_s}\varphi_{\mathrm{NL}}(i)\right)^2}. \tag{5}$$

The given characteristic is employed to distinguish PSK modulation from QPSK in hierarchical-based classifiers.

The continuous wavelet transform (CWT) forms our fifth and sixth attributes. CWT is based on the time-frequency analysis/conversion and is as follows [32]:

$$CWT_x^{\psi}(\tau, s) = \psi_x^{\psi}(\tau, s) = \int_{-\infty}^{+\infty} x(t)\,\psi_{\tau,s}^*(t)\,dt, \tag{6a}$$

$$\psi_{\tau,s} \triangleq \frac{1}{\sqrt{|s|}}\psi\left(\frac{t-\tau}{s}\right), \tag{6b}$$

where τ is the transition parameter, s indicates the scale parameter, and $\psi^*(t)$ represents the complex conjugate of $\psi(t)$. Accordingly, the correlation between the received signal's wavelet transform and the patterns stashed in the system is computed. The wavelet transform-related simulations exploit the Haar function. By comparing the computed CWT to BASK and BFSK templates, our system can distinguish between BPSK, QPSK, BFSK, and 4-FSK modulations. Table 1 summarizes the role of the six presented features. The effectiveness and roles of the selected features are illustrated in the simulation results in Section IV. In the following, machine learning models and algorithms used in this work are examined.

TABLE 1. The presented features and their roles.

	Features	Output Classes	
		CLASS 1	CLASS 2
1	$M_{\varphi_{\mathrm{NL}}}$	BFSK, BPSK, 4-FSK, QPSK, 16QAM	BASK, 4-ASK
2	σ_z^2	BASK	4-ASK
3	$\overline{\gamma}$	16QAM	BFSK, BPSK, 4-FSK, QPSK
4	σ_{dp}	BPSK	QPSK
5	CWT_BASK	BFSK, 4-FSK	BPSK, QPSK
6	CWT_BFSK	BFSK	4-FSK

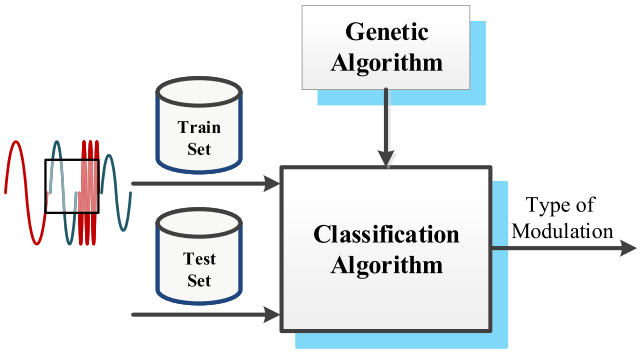

FIGURE 2. Flowchart of the proposed algorithm.

III. MACHINE LEARNING ALGORITHMS

As mentioned in previous sections, the main step in AMR is using machine learning-based classifier methods to accurately identify various modulation techniques. In our work, GA is utilized to acquire the optimal values of the tuning parameters of each method. The flowchart for the proposed model is illustrated in Fig. 2. Different artificial intelligence (AI) and machine learning [33] approaches based on ANNs and fuzzy logic (FL) systems are utilized for AMR. Trial-and-error approaches consume a vast amount of time and do not guarantee to achieve the optimal values. The proposed models require different and unique chromosome coding according to their structures and parameters. We define the tuning parameters of each algorithm to be the genes forming the chromosomes. Our presented network architecture is flexible and can vary in contrast to previous studies in which the same topology is considered for all machine learning methods. The MLP, RBF, ANFIS, DT, and NB models are examined in the following subsections.

A. MULTI-LAYER PERCEPTRON (MLP) ALGORITHM

MLP is one of the well-known and most widely used feedforward subclasses of ANNs in which the learning process is accomplished by employing multilayers of neurons. MLP models utilize the error back-propagation (EBP) technique [34], one of the well-known training schemes utilized to maximize network accuracy and achieve a superior outcome. The exact mathematical expression for calculating

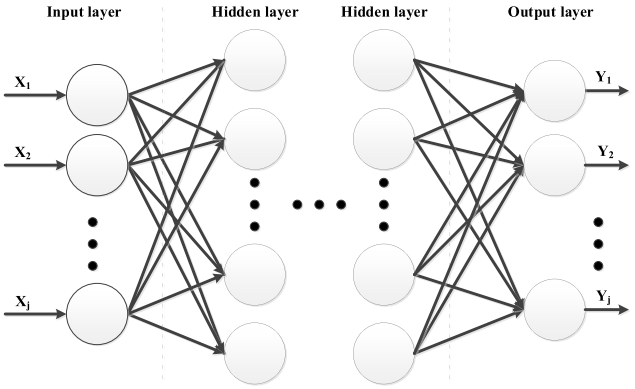

FIGURE 3. The MLP algorithm diagram.

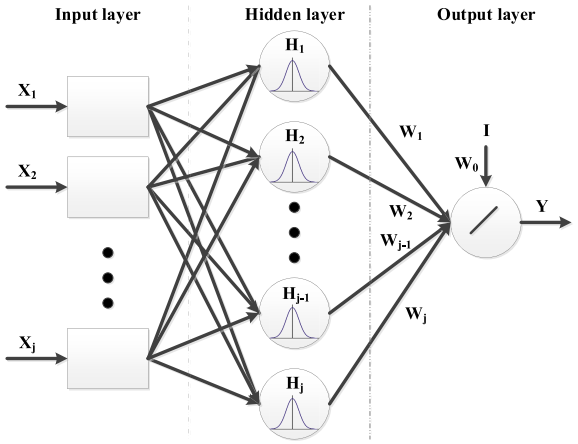

FIGURE 4. The three-layer feedforward structure of the RBF algorithm.

the error is

$$E = \frac{1}{2}\sum_{k=1}^{p}\sum_{i=1}^{M}(Z_i(k) - Y_i(k))^2, \tag{7}$$

where p denotes the number of training data, M represents the number of output neurons, Z_i is the actual output, and Y_i indicates the model output. Fig. 3 depicts the overall structure of the MLP network. It is worth noting that the hidden layers are not constrained to a specific number.

B. RADIAL BASIS FUNCTION (RBF) NETWORK

The RBF algorithms are another subclass of ANNs that possess a structure with three connected layers using feedforward connections. The existing neurons in the hidden layers of an RBF network employ radial basis functions such as Gaussian functions as the activation function [35]. The multi-layer structure of the RBF models is illustrated in Fig. 4. The mapping function that the RBF networks utilize is as follows [36]:

$$y = \sum_{j=1}^{N} w_j H_j(x), \tag{8a}$$

$$H_j(x) = \exp\left(-\frac{\left(\|x - c_j\|\right)^2}{2{\sigma_j}^2}\right), \tag{8b}$$

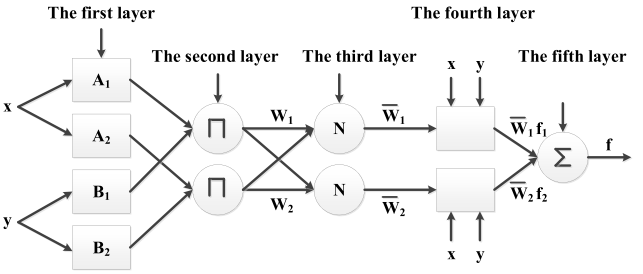

FIGURE 5. The 5-layer structure of the ANFIS algorithm.

where N represents the total number of hidden neurons, w_j denotes the weight allocated to the j^{th} node, $H_j(x)$ is the activation function of node j, $x \in [x_1, x_2, \ldots, x_j]$ represents the input given to the algorithm, c_j denotes the center of the j^{th} activation function, and σ_j indicates the smoothing parameter.

C. ADAPTIVE NEURO-FUZZY INFERENCE SYSTEM (ANFIS)

ANFIS is well recognized as an outstanding neuro-fuzzy model that concurrently utilizes FL and NN methods [37]. In fuzzy systems, the main features of the inference system and the tuning parameters have to be adjusted, which usually results in high computational complexity and is very time-consuming. Therefore, NNs are employed to prevail over the existing complications by tuning the adjustable parameters. This cooperation of the NNs and FL forms the neuro-fuzzy systems. Fig. 5 shows the five-layer structure of the Takagi-Sugeno-based ANFIS algorithm. The ANFIS models acquire their actual outputs using the following formula:

$$O_i = \sum_{i=1}^{n} \overline{w_i} f_i = \frac{\sum_{i=1}^{n} w_i f_i}{\sum_{i=1}^{n} w_i}, \tag{9}$$

where n denotes the total number of nodes, w_i represents the firing strengths of the rule layer, f_i indicates the first order polynomial with consequence parameters set of $\{p_i, q_i, r_i\}$, and $\overline{w_i}$ is the output of the normalization layer.

D. DECISION TREE (DT) ALGORITHM

DT is one of the most widely used data mining algorithms [38]. The DT is used in problems that can be posed in such a way that they provide a single answer in the form of a group or class name. There are many algorithms for constructing DTs; one of the most popular methods in this field is Iterative Dichotomiser 3 (ID3) [33]. In this algorithm, the tree is constructed from top to bottom. Entropy (E) and information gain (IG) criteria (using entropy to calculate the desired criterion) are used to find the best feature. The entropy or uncertainty of one system is calculated as follows:

$$E(S) = -p_+ \log_2 p_+ - p_- \log_2 p_-, \tag{10a}$$

$$E(S) = -\sum_{x \in X} p(x) \log_2 p(x), \tag{10b}$$

where S is the set of instances, p_+ represents the positive samples in S, and p_- indicates the negative samples in S.

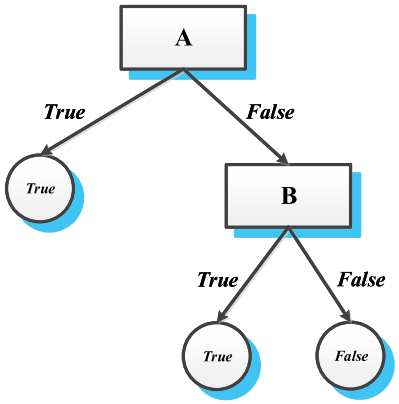

FIGURE 6. Flow diagram of a DT based on ID3.

The IG or the expected reduction in entropy by splitting the data on one attribute is defined as

$$\mathrm{IG}(S, A) = E(S) - \sum_{v \in \mathrm{Values}(A)} \frac{S_v}{S} E(S_v), \tag{11}$$

where the set Values(A) contains all possible values for attribute A. The set S_v is a subset of S whose characteristic A is equal to v. The general structure of the DT for a hypothetical data set containing two properties, A and B, is depicted in Fig. 6.

E. NAÏVE BAYES (NB) ALGORITHM

In machine learning, the NB algorithm is a group of simple classifiers based on probabilities. A simple Bayesian classifier can be considered as a model based on conditional probability. Suppose $X = (x_1, x_2, \ldots x_n)$ is a vector expressing n properties that are independent variables. Therefore, the probability of the occurrence of C_k, i.e., $p(C_k|x_1, x_2, \ldots x_n)$, can be represented as one of the states of various event classes for distinct k, as calculated below

$$p(C_k|X) = \frac{p(C_k)\, p(X|C_k)}{p(X)}. \tag{12}$$

Now, if each variable is assumed to be independent of the other variables, provided that the C_k category is independent, then the following equations are obtained:

$$p(x_i|x_{i+1}, \ldots, x_x, C_k) = p(x_i|C_k), \tag{13}$$

and

$$C = \underset{c_j}{argmax}\, p(C_k) \prod_i p(x_i|C_k). \tag{14}$$

An example of a two-dimensional data set is illustrated in Fig. 7.

The presented methods possess various tuning parameters that significantly impact the convergence, accuracy, and speed of the AMR system. Different approaches exist to determine the proper values of the tuning parameters. However, it is worth mentioning that some of the utilized algorithms are single-parameter, and therefore there is no need to use optimization algorithms. Trial-and-error is the most primitive technique to adjust the tuning parameter. Nevertheless, employing various optimization methods such as GA [39] is more effective to obtain the appropriate values of the parameters. In the following subsection, various GA coding schemes are proposed and examined to determine the optimal parameters of each model.

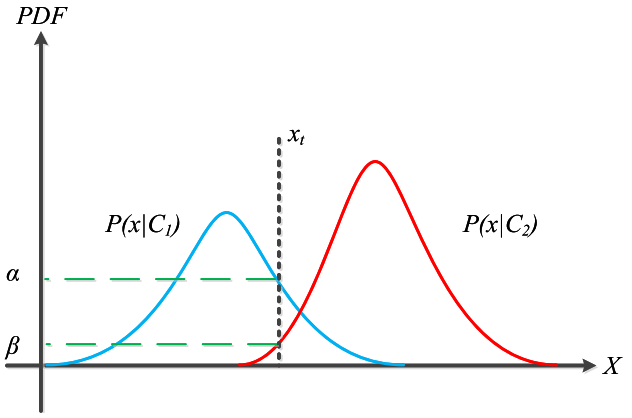

FIGURE 7. Hypothetical probability density functions (PDF).

F. GENETIC ALGORITHM (GA)

Optimization techniques consist of the two general categories of classical and modern approaches [40]. The classical optimization methods benefit from the damped least-squares (DLS) algorithm, while modern ones employ natural evolution processes. In addition, the former attains the local optimum, whereas the latter always aims to acquire the global optimum. As stated earlier, we employ GA in this study to optimize the tunable parameters of the presented machine learning algorithms. GA is a well-known modern method of optimization which Holland introduced in the 1970s [41]. Inspired by the principles of natural and gradual evolution (Darwin's theory), GA tries to discover an optimal solution in a vast searching space.

This algorithm conveys inherited traits through genes; however, these transitions of genes from one generation to another always face some variations. The crossover and mutation operations are two chief modifications that the algorithm applies to the genes and chromosomes. The presented GA leverages the crossover and mutation operators to merge and produce new chromosomes in order to achieve the global optimum [42], [43]. Additionally, a fitness (merit) function is defined to detect or acquire the best chromosome according to the requirements and demands. Fig. 8 illustrates the process flow and general structure of the GA.

Providing proper coding to define chromosomes is a critical step in GA. The presented algorithms, in addition to the weight coefficients, possess other adjustable parameters, including the type of fuzzy inference system (FIS), the number of membership functions, and the number of epochs in the ANFIS algorithm, learning rate, the number of epochs (iteration), and the network topology for the MLP model, the number of neurons in the hidden layer, the spread

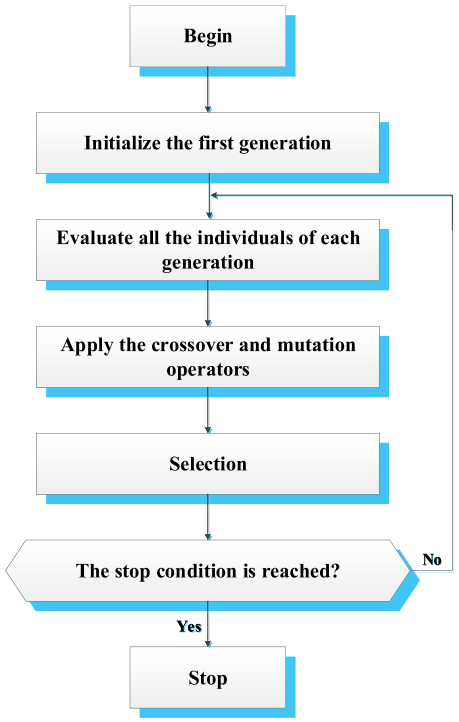

FIGURE 8. The general structure and process flow of the GA.

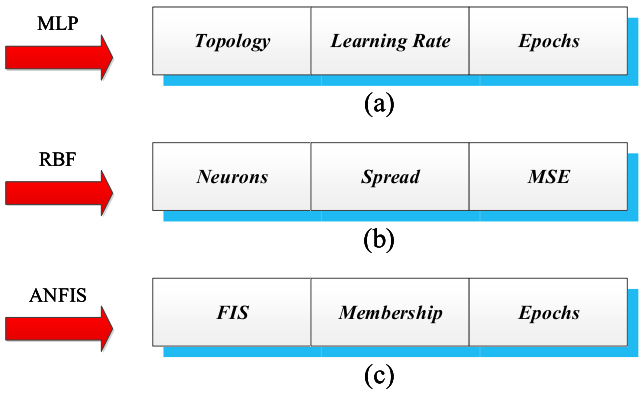

FIGURE 9. Chromosome structure formation for optimal parameter detection. a) MLP algorithm, b) RBF algorithm, c) ANFIS algorithm.

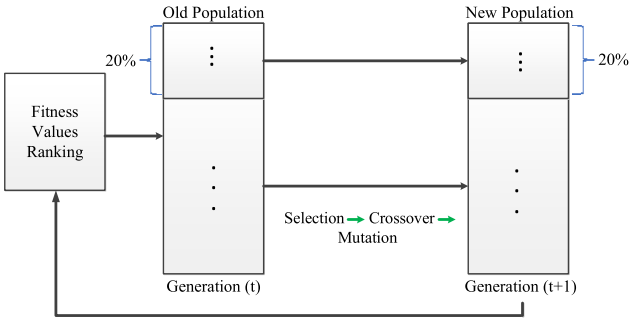

FIGURE 10. The proposed algorithm procedure for the production of new generations.

value, the mean squared error (MSE) factor of the RBF network. Improper designation of the tunable parameters of these models directly affects their convergence rate and computational load; therefore, proper values must be detected and assigned to them.

In light of the above, we first design appropriate codings for each of the presented models separately. The chromosomes and their constituent genes are determined according to the adjustable parameters of machine learning models in the proposed codings. Next, the model evaluates each chromosome by assessing the accuracy obtained for the algorithm employed in the AMR system. Ultimately, the fittest chromosomes, i.e., optimal parameters of the algorithms, are acquired. It is worth noting that the length of the chromosomes for all the models is constant; however, the types of genes forming a chromosome differ from one to the other. Fig. 9 illustrates the genes and chromosomes defined for each of the presented models, i.e., the parameters that the GA intends to optimize. Once the chromosome type is defined, the algorithm proceeds to elect the primary population.

If a small initial population is assigned for the system, the GA will be impotent to investigate the entire search space. In contrast, a large initial population decelerates the model. Consequently, we must select this quantity attentively. Given the restrictions associated with each component, the initial generation of the model is shaped by randomly generating 30 chromosomes [39]. The chromosomes of our GA have a structure similar to Fig. 9, the values of which for the first generation can be selected based on prior knowledge. As mentioned earlier, we randomly choose the initial values of the genes in this work. Random selection of the initial population empowers the algorithm to avoid getting trapped on a local optimum.

Afterward, the GA reproduces the next generation by executing the crossover and mutation operations. Fig. 10 demonstrates all the processes involved in creating a new generation. The proposed GA model utilizes single-point crossover with the probability of p_c exchanging parts of two single chromosomes. The mutation operator with the likelihood of p_m alters the gene value in some randomly selected chromosome locations assisting the model in avoiding loss of genetic diversity. Consequently, after several consecutive reproductions, the unfit chromosomes become extinct, while the best able to survive gradually dominate the population. Once the crossover and mutation processes are over, the model evaluates and picks out the best chromosomes among the offspring and parents in the selection phase to produce the next generation.

Our proposed algorithm sets the number of new descendants greater than the number of parents. The elitism strategy is employed in the selection stage to elect the fittest children and parents. This work utilizes the roulette wheel selection operator [44], which first calculates the fitness function value of each chromosome and then normalizes the computed results. The fitness function considered for each algorithm is the accuracy value that the algorithm calculates for each chromosome. The algorithm assigns a random number

between zero and one to each chromosome and calculates the probability of selecting that specific chromosome (P_i). Eventually, the most appropriate chromosome is chosen. Applying the above technique facilitates the selection of the chromosomes with a greater fitness level. The exact mathematical formula for the corresponding chromosome P_i value is

$$P_i = \frac{F_i}{\sum_{j=1}^{n} F_j}, \tag{15}$$

where F_i denotes the relevant fitness value of each chromosome, and n indicates the population number. We appoint appropriate values to the other two variables parameters: the occurrence probabilities of crossover and mutation operators (p_c and p_m). Once GA implements selection, crossover, and mutation operators, the model evaluates the fitness function and gradually achieves the optimized parameters for the selected machine learning models by enhancing the fitness value. The performance of the presented GA and the relative efficiency of the MLP, RBF, ANFIS, DT, NB algorithms in AMR is investigated.

IV. SIMULATION RESULTS

We perform several experimental studies in this section to evaluate the performance of the proposed methods. The simulations are executed in MATLAB 2020a equipped with NN toolboxes. The AWGN channel is considered for the communication system. Therefore, once the transmitter modulates and then conveys the signal through the channel, the transmitted signal is mixed with white Gaussian noise. The transmitted signal then arrives at the receiver block, where no prior information from the transmitter exists. Information regarding the proposed algorithms and utilized signal parameters is summarized in Table 2. The efficiency and performance of the proposed models are investigated by considering different criteria. We first examine the selected features and their role by performing various simulations in the following subsection.

A. SELECTED FEATURES

The employed features are briefly studied earlier in the system model and selected features in Section II. As illustrated in Fig. 11, the ASK-modulated signals obtain the lowest values after considering the second-order moment of the non-linear component of the instantaneous phase ($M_{\varphi_{\mathrm{NL}}}$), i.e., our first feature, which helps to separate ASK modulations from other schemes. Fig. 12 depicts that the spectrum-based feature (σ_z^2) can accurately distinguish ASK and QAM modulations from other digital modulations schemes, including PSK and FSK modulations that possess no amplitude-related information. The proposed AMR models of this study utilize the mean value of the power spectral density of the normalized-centered instantaneous amplitude of the intercepted signal segment ($\overline{\gamma}$) to detach 4-ASK modulations from BASK, as demonstrated in Fig. 13.

TABLE 2. Assumptions of input signal parameters and proposed algorithms.

	Parameters	Values
1	Sampling Frequency	1200 KHz
2	Carrier Frequency	150 KHz
3	Symbol Rate	12.5 KHz
4	Number of Modulations	7
5	Number of Samples	7×3600
6	Continuous Wavelet Transform	Haar Function with 64 Scale Values
7	K in KNN	5
8	Smoothing Parameter in PNN	0.1
9	Topology in MLP	$[7 - 20 - 6]$
10	LR in MLP	0.2
11	Epochs in MLP	80
12	Neurons in RBF	300
13	Spread in RBF	0.9
14	MSE in RBF	0.1
15	FIS in ANFIS	*genfis2*
16	Membership in ANFIS	-
17	Epochs in ANFIS	80
18	DT	-
19	NB Distribution	*Normal* Distribution

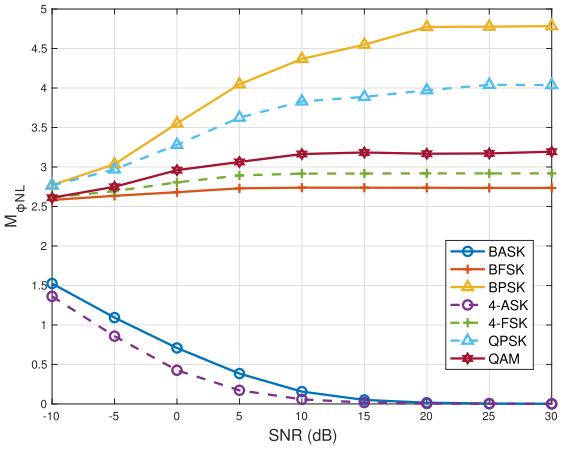

FIGURE 11. The values obtained for various types of modulated signals with respect to the first feature versus SNR.

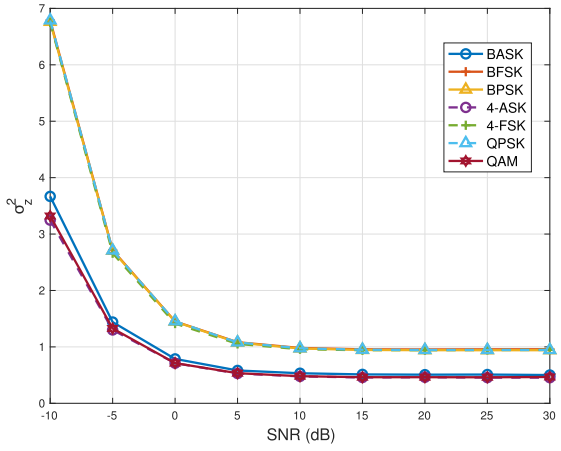

FIGURE 12. The values obtained for various types of modulated signals with respect to the second feature versus SNR.

As shown in Fig. 14, the standard deviation of the normalized-centered non-linear component of the direct

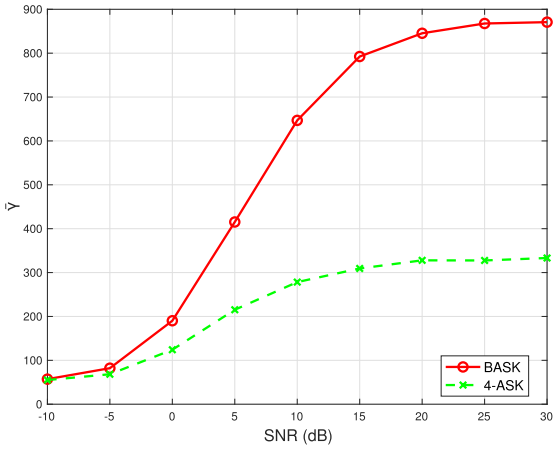

FIGURE 13. The values obtained for various types of modulated signals with respect to the third feature versus SNR.

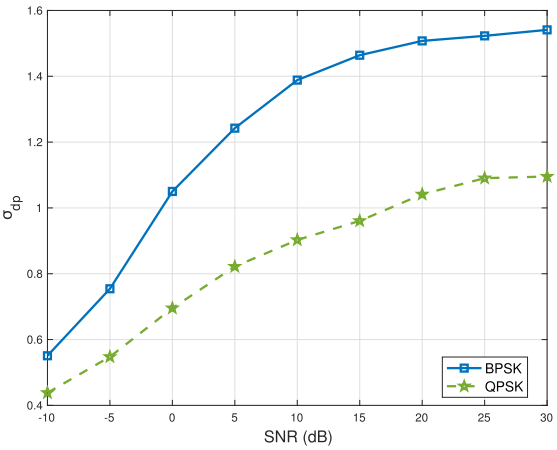

FIGURE 14. The values obtained for various types of modulated signals with respect to the fourth feature versus SNR.

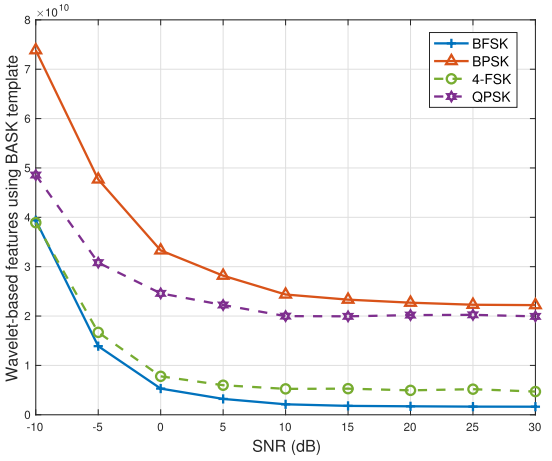

FIGURE 15. The values obtained for various types of modulated signals with respect to the fifth feature versus SNR.

instantaneous phase (σ_{dp}) is employed to distinguish PSK modulation from QPSK in hierarchical-based classifiers.

Figs. 15 and 16 illustrate how the CWT-based features empower our model to recognize BPSK, QPSK, BFSK, and 4-FSK modulations schemes.

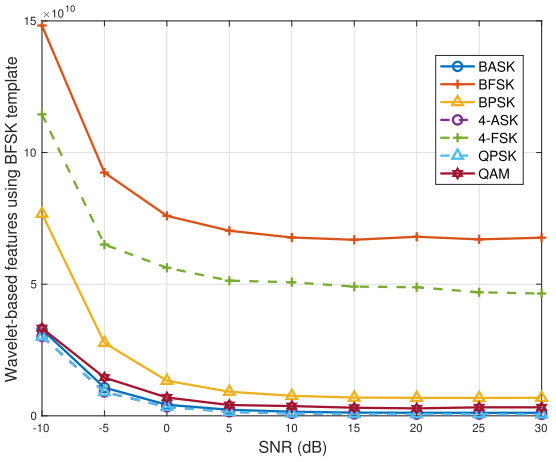

FIGURE 16. The values obtained for various types of modulated signals with respect to the sixth feature versus SNR.

B. EVALUATION AND COMPARISON METRICS

1) ACCURACY

The accuracies of the presented models are calculated as

$$\overline{Acc_i} = \frac{1}{m}\sum_{k=1}^{m}\frac{n_k}{n_i}, \tag{16}$$

where i is the SNR value, m indicates the number of iterations per SNR, n_i represents the total number of testing instances, and n_k denotes the total number of correctly classified digital modulation schemes.

2) SPEED COMPARISON AND EVALUATION

One of the essential evaluation criteria is the algorithm's speed in real-time applications, i.e., time complexity. Therefore, the computation times of the selected machine learning models are reported to provide a detailed comparison.

3) PARAMETERS EVALUATION AND CONFUSION MATRIX

Most of the studied algorithms have an adjustable parameter. Imprecise selection of tuning parameters, i.e., extremely small or large, diminishes the accuracy of the model. Therefore, the values of these parameters must be chosen appropriately. GAs are utilized in algorithms with a large number of parameters. In algorithms that have only one parameter, two approaches can be used. The first approach is to use the trial-and-error method. Furthermore, in the second tactic, the 10-fold cross-validation technique is employed to find values for the parameters.

In the M-fold cross-validation approach, the dataset samples are distributed into M different subsamples of the same size. In each step/iteration, the technique utilizes one of the M sets for evaluation purposes, while the rest are employed in the training process. Accordingly, the average error per p iterations is calculated as [45]

$$\overline{\varepsilon} = \frac{\sum_{i=1}^{p}\left(\frac{\sum_{j=1}^{M}(Error\_Fold_j)}{M}\right)}{p}. \tag{17}$$

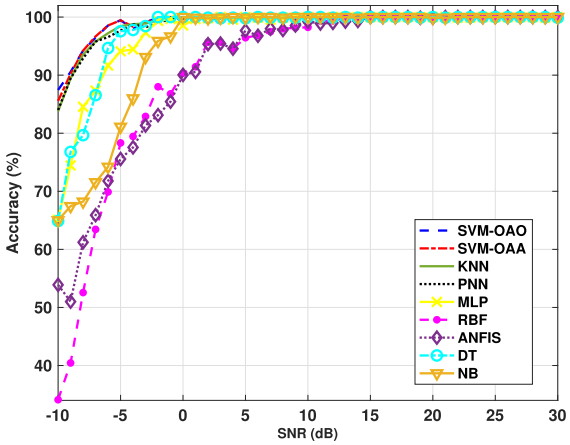

FIGURE 17. Accuracy comparison of the AMR algorithms.

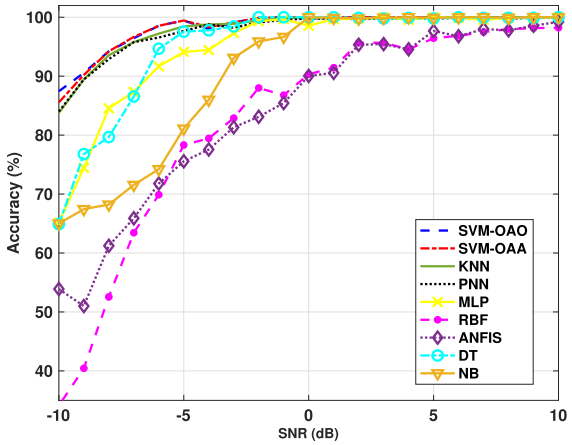

FIGURE 18. Comparison of the models performance at SNRs −10 dB to 10 dB.

We compare the results of our proposed models with other studies, in particular [9], [32], and [46]. The work in [9] and [32] propose a hierarchy-based support vector machine (SVM) classifier. The authors investigate the two approaches, namely one against one (OAO) and one against all (OAA). The study in [46] employs probabilistic neural network (PNN) and KNN algorithms for AMR. In these work, a total of six features are exploited to recognize seven different digital modulation schemes. Fig. 17 compares the performance of the proposed methods versus different SNRs. Our proposed models provide robust modulation recognition with high accuracy at very low SNRs, i.e., extremely noisy environments. In particular, it is seen that the MLP and DT methods achieve an accuracy of above 95% at an SNR of −6 dB. Moreover, all the utilized algorithms provide accuracies greater than 90% at SNR = 0 dB.

In addition, to better compare the performance of the models, Fig. 18 shows the related accuracies of all the algorithms at different SNRs ranging from −10 dB up to 10 dB. The figure provides better visualization of the accuracies obtained by the proposed models. The overlapping lines indicate that the distinct machine learning algorithms achieve similar accuracy at specific SNRs. Most of our employed algorithms, including MLP, DT, and NB, achieve an accuracy of 100% at the SNR of 0 dB.

The average accuracy obtained from 30 realizations of simulation per SNR is given in these simulations. Table 3 provides a comparison made for a specific SNR equal to 0 dB. Our proposed models result in significantly faster and more efficient AMR without compromising the accuracy. In particular, the presented DT offers 96.75% speedup over SVM-OAO and 89.13% over SVM-OAA. Other employed models of this study provide an average speedup of 89% and 65% over SVM-OAO and SVM-OAA, respectively. As observed, the DT algorithm consumes the least time to provide a suitable output. Providing the correct result in the shortest possible time facilitates the use of the proposed algorithms in real-time applications. Table 4 lists the associated accuracy for various SNRs. In addition, this

TABLE 3. The speed and accuracy performance of the presented algorithms at SNR = 0 dB.

	References	Time (s)	Accuracy (%)
1	MLP	3.0631	100
2	RBF	5.4198	90.33
3	ANFIS	4.7347	90.24
4	DT	1.4219	100
5	NB	7.5923	100
6	KNN	5.0187	100
7	PNN	7.6358	100
8	SVM-OAO	43.7982	100
9	SVM-OAA	13.0852	100

table contains the results of some other related studies. In the methods proposed in the comparable studies, various machine learning and AI techniques are employed. As can be observed, the presented techniques, even at low SNRs, successfully offer very high accuracy. In particular, the proposed DT, MLP, and NB algorithms provide 100%, 99.66%, and 96.66% accuracy at SNR = −2 dB, respectively.

One of the most significant achievements of the presented study is using single-parameter methods in which trial-and-error methods obtain the optimal parameter value. Using algorithms with a minimum number of parameters will increase the speed of machine learning algorithms in the training and testing process. Moreover, for multi-parameter models, it can be mentioned that the specific GA presented in this work is utilized to find the optimal values of the parameters for these approaches.

The GA exploiting the 10-fold cross-validation technique is employed to obtain the optimal values of the adjustable parameters. Figs. 19 and 20 examine the accuracies of the MLP and RBF models with respect to changes in the values of the tunable parameters, respectively. We observe that the appropriate selection of adjustable parameters values significantly improves the performance of the proposed models. It is clearly seen that the optimal selection of these parameters significantly improves the performance of the employed models (up to 70%).

TABLE 4. Performance comparison of various digital modulation recognition techniques.

	References	Modulations	SNR (dB)	Accuracy (Percentage %)
1	Presented MLP	BASK, 4-ASK, BFSK, 4-FSK, BPSK, 4-PSK, 16-QAM	-2	99.66
2	Presented RBF	BASK, 4-ASK, BFSK, 4-FSK, BPSK, 4-PSK, 16-QAM	-2	88.00
3	Presented ANFIS	BASK, 4-ASK, BFSK, 4-FSK, BPSK, 4-PSK, 16-QAM	-2	85.44
4	Presented DT	BASK, 4-ASK, BFSK, 4-FSK, BPSK, 4-PSK, 16-QAM	-2	100
5	Presented NB	BASK, 4-ASK, BFSK, 4-FSK, BPSK, 4-PSK, 16-QAM	-2	96.66
6	KNN in [46]	BASK, 4-ASK, BFSK, 4-FSK, BPSK, 4-PSK, 16-QAM	-2	100
7	PNN in [46]	BASK, 4-ASK, BFSK, 4-FSK, BPSK, 4-PSK, 16-QAM	-2	99.60
8	[26]	BPSK, QPSK, 8-PSK	-1	75.99
9	[29]	ASK, FSK, PSK, QASK, QFSK, QPSK	0	99.19
10	[47]	BASK, BFSK, 4-FSK, 8-FSK, BPSK, 4-PSK, 16-QAM, 32-QAM, 64-QAM	0	100
11	[48]	BPSK, 4-PSK, 8-PSK	-1	99.00
12	[49]	BFSK, 4-FSK, BPSK, 4-PSK, 8-PSK	9	92.60
13	[50]	BASK, 4-ASK, BFSk, 4-FSK, BPSK, 4-PSK, 16-QAM	5	97.00
14	[7]	BASK, 4-ASK, BFSK, 4-FSK, BPSK, 4-PSK, 8-PSK	10	86.50
15	[51]	BPSK, 4-PSK, 16-QAM, 64-QAM	4	89.40
16	[13]	BASK, 4-ASK, BFSK, 4-FSK, BPSK, 4-PSK, MSK, 16-QAM	10	95.00
17	[19]	BPSK, 8-PSK, 4-ASK, 16-QAM	0-35	100
18	[25]	BPSK, QPSK, 8-PSK, BASK, 4-ASK, 4-QAM, 16-QAM, 32-QAM, 64-QAM	0-35	99.06
19	[52]	BASK, QPSK, 16-QAM	0-35	99.83

Furthermore, it is observed that the DT classifier has the least computation time. Accordingly, to further study the model, Table 5 lists the results obtained for this algorithm at SNR $= -6$ dB in the form of a confusion matrix. The confusion matrix reports the prediction results of our model.

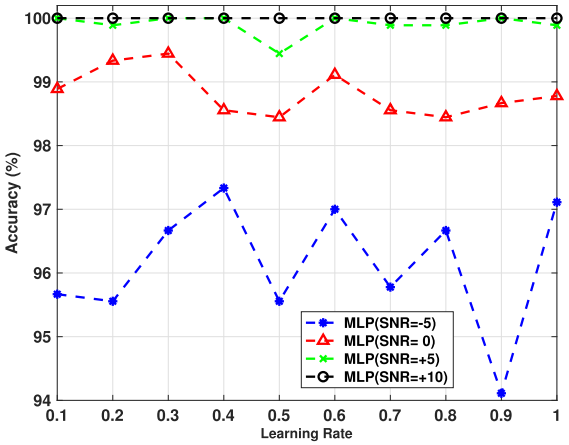

FIGURE 19. The accuracy of the MLP at different SNRs (−5 dB, 0 dB, 5 dB, 10 dB) plotted versus the learning rate parameter.

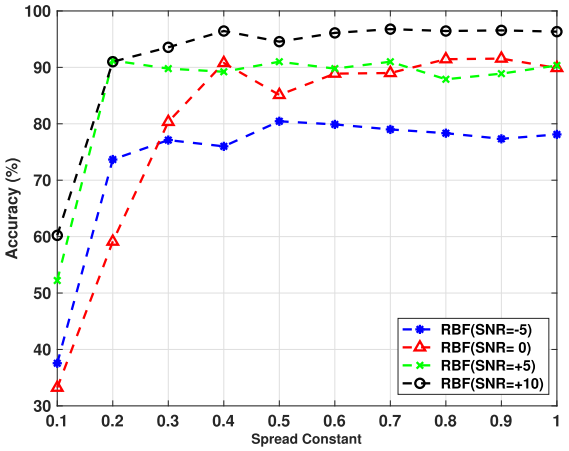

FIGURE 20. The accuracy of the RBF at different SNRs (−5 dB, 0 dB, 5 dB, 10 dB) plotted versus the spread value parameter.

TABLE 5. DT algorithm confusion matrix results at SNR $= -6$ dB (Test Data = 900; Approximately 128 for each modulation scheme).

Confusion Matrix	BASK	4-ASK	BFSK	4-FSK	BPSK	4-PSK	16-QAM
BASK	124	2			2		
4-ASK	3	123				2	
BFSK			120	6		2	
4-FSK		2		124	2		
BPSK	2			5	120	1	
4-PSK			1			126	1
16-QAM					1	3	124

The number of correct and incorrect predictions are listed for each modulation scheme. As can be concluded from the figures and tables above, the proposed models provide excellent accuracy.

V. CONCLUSION

MLP, RBF, ANFIS, DT, and NB models are leveraged in this study to intelligently detect and classify numerous digital modulation schemes based on the presented key features. Additionally, we exploit a heuristic optimization method, namely GA, to determine the optimal values of the tunable parameters for the machine algorithms. The

simulation results illustrate that the proposed algorithms have superior accuracy while employing significantly fewer classifiers, parameters, and computations. It is observed that the selected models successfully identify and classify the received signals that have been modeled in different ways in a short time and with extreme accuracy. Furthermore, the presented approaches substantially elevate the speed of the AMR system, in particular up to 96.75% improvement compared to previous studies. These classical methods can compete reasonably well with deep learning algorithms. It can also be stated that algorithms can accurately and robustly identify the signal modulation schemes received at extremely low SNRs. Various channel types, including Rayleigh and Rician fading, can be investigated in the future to extend the work. In addition, it should be noted that the hardware aspect of the methods should also be evaluated as future work.

REFERENCES

[1] Z. Zhu and A. K. Nandi, *Automatic Modulation Classification: Principles, Algorithms and Applications*. Hoboken, NJ, USA: Wiley, 2015.
[2] B. Jdid, K. Hassan, I. Dayoub, W. H. Lim, and M. Mokayef, "Machine learning based automatic modulation recognition for wireless communications: A comprehensive survey," *IEEE Access*, vol. 9, pp. 57851–57873, 2021.
[3] O. A. Dobre, A. Abdi, Y. Bar-Ness, and W. Su, "Survey of automatic modulation classification techniques: Classical approaches and new trends," *IET Commun.*, vol. 1, no. 2, pp. 137–156, Apr. 2007.
[4] I. Abdel Hafiz El Rube and N. El-din El-Madany, "Cognitive digital modulation classifier using artificial neural networks for NGNs," in *Proc. 7th Int. Conf. Wireless Opt. Commun. Netw. (WOCN)*, Sep. 2010, pp. 1–5.
[5] J. L. Xu, M. Zhou, and W. Su, "Discrete likelihood ratio test for intelligent signal recognition in software defined radio," in *Proc. 19th Annu. Wireless Opt. Commun. Conf. (WOCC)*, May 2010, pp. 1–6.
[6] P. Prakasam and M. Madheswaran, "Modulation identification algorithm for adaptive demodulator in software defined radios using wavelet transform," *Int. J. Signal Process.*, vol. 5, no. 1, pp. 74–81, 2009.
[7] W. Su, Z. Lei, H. Li, and T. Han, "The research of modulation recognition algorithm base on softwore radio," in *Proc. 2nd Int. Conf. Comput. Eng. Technol.*, vol. 7, Apr. 2010, pp. V7–308.
[8] E. Azzouz and A. K. Nandi, *Automatic Modulation Recognition of Communication Signals*. Springer, 2013.
[9] S. Hassanpour, A. M. Pezeshk, and F. Behnia, "Automatic digital modulation recognition based on novel features and support vector machine," in *Proc. 12th Int. Conf. Signal-Image Technol. Internet-Based Syst. (SITIS)*, Nov./Dec. 2016, pp. 172–177.
[10] S.-Z. Hsue and S. S. Soliman, "Automatic modulation classification using zero crossing," *IEE Proc. F (Radar Signal Process.)*, vol. 137, no. 6, pp. 459–464, 1990.
[11] F. F. Liedtke, "Computer simulation of an automatic classification procedure for digitally modulated communication signals with unknown parameters," *Signal Process.*, vol. 6, no. 4, pp. 311–323, Aug. 1984.
[12] K. Hassan, I. Dayoub, W. Hamouda, and M. Berbineau, "Automatic modulation recognition using wavelet transform and neural networks in wireless systems," *EURASIP J. Adv. Signal Process.*, vol. 2010, no. 1, pp. 1–13, Dec. 2010.
[13] C.-S. Park, J.-H. Choi, S.-P. Nah, W. Jang, and D. Y. Kim, "Automatic modulation recognition of digital signals using wavelet features and SVM," in *Proc. 10th Int. Conf. Adv. Commun. Technol.*, vol. 1, Feb. 2008, pp. 387–390.
[14] M. P. DeSimio and G. E. Prescott, "Adaptive generation of decision functions for classification of digitally modulated signals," in *Proc. IEEE Nat. Aerosp. Electron. Conf.*, May 1988, pp. 1010–1014.
[15] S. Kharbech, I. Dayoub, M. Zwingelstein-Colin, E. P. Simon, and K. Hassan, "Blind digital modulation identification for time-selective MIMO channels," *IEEE Wireless Commun. Lett.*, vol. 3, no. 4, pp. 373–376, Aug. 2014.
[16] A. Ebrahimzadeh and R. Ghazalian, "Blind digital modulation classification in software radio using the optimized classifier and feature subset selection," *Eng. Appl. Artif. Intell.*, vol. 24, no. 1, pp. 50–59, 2011.
[17] X. Zhang, J. Sun, and X. Zhang, "Automatic modulation classification based on novel feature extraction algorithms," *IEEE Access*, vol. 8, pp. 16362–16371, 2020.
[18] A. K. Nandi and E. E. Azzouz, "Algorithms for automatic modulation recognition of communication signals," *IEEE Trans. Commun.*, vol. 46, no. 4, pp. 431–436, Apr. 1998.
[19] T. A. Almohamad, M. F. M. Salleh, M. N. Mahmud, A. H. Y. Sa'd, and S. A. Al-Gailani, "Automatic modulation recognition in wireless communication systems using feature-based approach," in *Proc. 10th Int. Conf. Robot., Vis., Signal Process. Power Appl.* Singapore: Springer, 2019, pp. 403–409.
[20] M. L. D. Wong and A. K. Nandi, "Automatic digital modulation recognition using artificial neural network and genetic algorithm," *Signal Process.*, vol. 84, no. 2, pp. 351–365, 2004.
[21] Z. Zhu, M. Waqar Aslam, and A. K. Nandi, "Augmented genetic programming for automatic digital modulation classification," in *Proc. IEEE Int. Workshop Mach. Learn. Signal Process.*, Aug. 2010, pp. 391–396.
[22] L. Zhang, L. B. Jack, and A. K. Nandi, "Extending genetic programming for multi-class classification by combining K-Nearest neighbor," in *Proc. IEEE Int. Conf. Acoust., Speech, Signal Process. (ICASSP)*, vol. 5, Mar. 2005, pp. V–349.
[23] N. Ghani and R. Lamontagne, "Neural networks applied to the classification of spectral features for automatic modulation recognition," in *Proc. IEEE Mil. Commun. Conf. (MILCOM)*, vol. 1, Oct. 1993, pp. 111–115.
[24] K. Neshatian and M. Zhang, "Genetic programming for performance improvement and dimensionality reduction of classification problems," in *Proc. IEEE Congr. Evol. Comput. (IEEE World Congr. Comput. Intell.)*, Jun. 2008, pp. 2811–2818.
[25] T. A. Almohamad, M. F. M. Salleh, M. N. Mahmud, I. R. Karas, N. S. M. Shah, and S. A. Al-Gailani, "Dual-determination of modulation types and signal-to-noise ratios using 2D-ASIQH features for next generation of wireless communication systems," *IEEE Access*, vol. 9, pp. 25843–25857, 2021.
[26] K. Jiang, J. Zhang, H. Wu, A. Wang, and Y. Iwahori, "A novel digital modulation recognition algorithm based on deep convolutional neural network," *Appl. Sci.*, vol. 10, no. 3, p. 1166, Feb. 2020.
[27] W. Xie, S. Hu, C. Yu, P. Zhu, X. Peng, and J. Ouyang, "Deep learning in digital modulation recognition using high order cumulants," *IEEE Access*, vol. 7, pp. 63760–63766, 2019.
[28] M. Zhang, Y. Zeng, Z. Han, and Y. Gong, "Automatic modulation recognition using deep learning architectures," in *Proc. IEEE 19th Int. Workshop Signal Process. Adv. Wireless Commun. (SPAWC)*, Jun. 2018, pp. 1–5.
[29] N. Daldal, Z. Cömert, and K. Polat, "Automatic determination of digital modulation types with different noises using convolutional neural network based on time–frequency information," *Appl. Soft Comput.*, vol. 86, Jan. 2020, Art. no. 105834.
[30] T. Zhang, C. Shuai, and Y. Zhou, "Deep learning for robust automatic modulation recognition method for IoT applications," *IEEE Access*, vol. 8, pp. 117689–117697, 2020.
[31] J. Proakis and M. Salehi, *Communication Systems Engineering*. Upper Saddle River, NJ, USA: Prentice-Hall, 2002.
[32] S. Hassanpour, A. M. Pezeshk, and F. Behnia, "A robust algorithm based on wavelet transform for recognition of binary digital modulations," in *Proc. 38th Int. Conf. Telecommun. Signal Process. (TSP)*, Jul. 2015, pp. 508–512.
[33] J. R. Quinlan, *Programs for Machine Learning*. Amsterdam, The Netherlands: Elsevier, 2014, Ch. 4. 5.
[34] S.-H. Oh, "Error back-propagation algorithm for classification of imbalanced data," *Neurocomputing*, vol. 74, no. 6, pp. 1058–1061, Feb. 2011.
[35] T. Chen and H. Chen, "Approximation capability to functions of several variables, nonlinear functionals, and operators by radial basis function neural networks," *IEEE Trans. Neural Netw.*, vol. 6, no. 4, pp. 904–910, Jul. 1995.
[36] V. Nekoukar and M. T. Hamidi Beheshti, "A local linear radial basis function neural network for financial time-series forecasting," *Int. J. Speech Technol.*, vol. 33, no. 3, pp. 352–356, Dec. 2010.
[37] J.-S. R. Jang, "ANFIS: Adaptive-network-based fuzzy inference system," *IEEE Trans. Syst., Man, Cybern.*, vol. 23, no. 3, pp. 665–685, May/Jun. 1993.

[38] J. R. Quinlan, "Induction of decision trees," *Mach. Learn.*, vol. 1, no. 1, pp. 81–106, 1986.
[39] S. Ansari, K. A. Alnajjar, S. Abdallah, M. Saad, and A. A. El-Moursy, "Parameter tuning of MLP, RBF, and ANFIS models using genetic algorithm in modeling and classification applications," in *Proc. Int. Conf. Inf. Technol. (ICIT)*, Jul. 2021, pp. 660–666.
[40] I. Zelinka, V. Snasael, and A. Abraham, *Handbook of Optimization: From Classical to Modern Approach*, vol. 38. Springer, 2012.
[41] J. H. Holland, *Adaptation in Natural and Artificial Systems: An Introductory Analysis With Applications to Biology, Control, and Artificial Intelligence*. Cambridge, MA, USA: MIT Press, 1992.
[42] D. E. Goldberg, *Genetic Algorithms*. London, U.K.: Pearson, 2006.
[43] M. Negnevitsky, *Artificial Intelligence: A Guide to Intelligent Systems*. London, U.K.: Pearson, 2005.
[44] D. E. Goldberg, *Genetic Algorithms in Search, Optimization and Machine Learning*, 1st ed. Reading, MA, USA: Addison-Wesley, 1989.
[45] G. James, D. Witten, T. Hastie, and R. Tibshirani, *An Introduction to Statistical Learning*, vol. 112. Springer, 2013.
[46] S. Ansari, K. A. Alnajjar, S. Abdallah, and M. Saad, "Automatic digital modulation recognition based on machine learning algorithms," in *Proc. Int. Conf. Commun., Comput., Cybersecur., Informat. (CCCI)*, Nov. 2020, pp. 1–6.
[47] S. Jin, Y. Lin, and H. Wang, "Automatic modulation recognition of digital signals based on fisherface," in *Proc. IEEE Int. Conf. Softw. Qual., Rel. Secur. Companion (QRS-C)*, Jul. 2017, pp. 216–220.
[48] F. Xie, C. Li, and G. Wan, "An efficient and simple method of MPSK modulation classification," in *Proc. 4th Int. Conf. Wireless Commun., Netw. Mobile Comput.*, Oct. 2008, pp. 1–3.
[49] M. Zhou and Q. Feng, "A new feature parameter for MFSK/MPSK recognition," in *Proc. Int. Conf. Intell. Sci. Inf. Eng.*, Aug. 2011, pp. 21–23.
[50] J. Bagga and N. Tripathi, "Analysis of digitally modulated signals using instantaneous and stochastic features for classification," *Int. J. Soft Comput. Eng. (IJSCE)*, vol. 1, no. 2, pp. 2231–2307, 2011.
[51] M. W. Aslam, Z. Zhu, and A. K. Nandi, "Automatic modulation classification using combination of genetic programming and KNN," *IEEE Trans. Wireless Commun.*, vol. 11, no. 8, pp. 2742–2750, Aug. 2012.
[52] T. A. Almohamad, M. F. M. Salleh, M. Mahmud, and A. H. Y. Sa'd, "Simultaneous determination of modulation types and signal-to-noise ratios using feature-based approach," *IEEE Access*, vol. 6, pp. 9262–9271, 2018.

SAM ANSARI received the B.Sc. degree in telecommunication engineering from Canadian University Dubai, Dubai, United Arab Emirates, and the M.Sc. degree in electrical and computer engineering from Abu Dhabi University, Abu Dhabi, United Arab Emirates. He is currently pursuing the Ph.D. degree with the Department of Electrical and Computer Engineering, University of Sharjah, Sharjah, United Arab Emirates. His research interests include wireless communications, molecular communication, artificial intelligence, machine learning, and renewable energy.

KHAWLA A. ALNAJJAR (Member, IEEE) received the B.S. degree in electrical engineering, communication track from United Arab Emirates University (UAEU), Al Ain, in 2008, the M.S. and P.E.E. degrees in electrical engineering from Columbia University, New York, in 2010 and 2012, respectively, and the Ph.D. degree in electrical and electronics engineering from the University of Canterbury, Christchurch, New Zealand, in 2015. She is currently an Assistant Professor with the Department of Electrical and Computer Engineering, University of Sharjah, United Arab Emirates. Her research interests include wireless communication systems, mathematical statistics, and network information theory and power grids. She has received more than 30 competitive awards for her successful studies and research during these ten years.

MOHAMED SAAD (Senior Member, IEEE) received the Ph.D. degree in electrical and computer engineering from McMaster University, Hamilton, Canada, in 2004.

He held research positions with the Department of Electrical and Computer Engineering, University of Toronto, Toronto, Canada; and the Advanced Optimization Laboratory, Department of Computing and Software, McMaster University. He is currently a Professor with the Department of Computer Engineering, University of Sharjah, United Arab Emirates. His research interests include networking, communications and optimization, with current activity focused on the optimal design of wireless and wired communication networks, and optimal network resource management. He was a recipient of the 2005–2006 Natural Sciences and Engineering Research Council of Canada (NSERC) Postdoctoral Fellowship; two best teaching awards by the IEEE Women in Engineering Society, University of Sharjah, in 2007 and 2009; the Best Paper Award in the IEEE Symposium on Computers and Communications, Riccione, Italy, in June 2010; the Annual Incentive Award for Distinguished Faculty Members, for excellence in research from the University of Sharjah, in April 2010 (university-wide). He is an Associate Editor of *Frontiers in Communications and Networks*.

SAEED ABDALLAH (Member, IEEE) received the B.Eng. degree in computer and communications engineering from the American University of Beirut, Beirut, Lebanon, in 2005, and the M.Sc. and Ph.D. degrees in electrical engineering from McGill University, Montreal, QC, Canada, in 2008 and 2013, respectively. He is currently an Assistant Professor with the Department of Electrical and Computer Engineering, University of Sharjah, Sharjah, United Arab Emirates. His research interests include signal processing for wireless communications, with special emphasis on relay networks, multicarrier systems, MIMO and massive MIMO systems, Wi-Fi systems, channel estimation/prediction, and adaptive modulation.

ALI A. EL-MOURSY (Senior Member, IEEE) received the Ph.D. degree in high-performance computer architecture from the University of Rochester, Rochester, NY, USA, in 2005. He was with the Software Solution Group, Intel Corporation, CA, USA, until early 2007. In 2007, he joined the Electronics Research Institute, Giza, Egypt. He was also a Visitor Research Scientist with the IBM Cairo Technology Development Center, Egypt, from February 2007 to January 2010. In September 2010, he joined the Electrical and Computer Engineering Department, University of Sharjah, Sharjah, United Arab Emirates, as an Assistant Professor, where he promoted as an Associate Professor, in January 2017. His research interests include high-performance computer architecture, multi-core multi-threaded mirco-architecture, power-aware micro-architecture, simulation and modeling of architecture performance and power, workload profiling and characterization, cell programming, high performance computing, parallel computing, and cloud computing.